doi:10.4149/neo_2022_211205N1728

CX3CL1 in the red bone marrow promotes renal cell carcinoma to metastasize to the spine by involving the Src-related pathway

An-Nan HU#, Fan-Cheng CHEN#, Ke-Tao WANG#, Zhen-Qing WANG, Yun LIANG, Jian DONG*

Department of Orthopedic Surgery, Zhongshan Hospital, Fudan University, Shanghai, China

**Correspondence: dong.jian@zs-hospital.sh.cn*
#Contributed equally to this work.

Received December 5, 2021 / Accepted March 15, 2022

Spinal metastasis (SM) frequently occurs in renal cell carcinoma (RCC) patients. Our preliminary work showed that CX3CL1 plays a positive role in SM. The objective of the present study was to verify whether CX3CL1 activates the downstream pathway by binding to CX3CR1 in RCC cells, ultimately promoting RCC to metastasize to the spine. The expression of CX3CL1 and CX3CR1 in tissue samples was detected by immunohistochemistry and western blotting. ELISA was used to quantify the concentration of CX3CL1 in the serum. The expression level of CX3CR1 in RCC cell lines was also detected. The CellTiter-Glo assay and flow cytometry were used to analyze cell viability and apoptosis of RCC cells. Transwell and wound healing assay were used to analyze the effect of CX3CL1 on the invasion and migration ability of RCC cells. Specific inhibitors were used to interfere with key molecules in the signaling pathway to further explore the signal transduction in RCC cells after CX3CL1 stimulation. The expression of CX3CR1 in SM from RCC was higher than that in limb bone metastases. Among the five RCC cell lines, 786O cells expressed the highest level of CX3CR1. CX3CL1 neither inhibited the proliferation of 786O cells nor promoted the apoptosis of 786O cells. However, it promoted the migration and invasion of RCC cells. After CX3CL1 stimulation, Src and Focal adhesion kinase (FAK) phosphorylation levels increased in RCC cells. Bosutinib and PF-00562271 inhibited Src/FAK phosphorylation and cell motility and invasion triggered by CX3CL1 stimulation. CX3CL1 in the red bone marrow of spinal cancellous bone enhances migration and invasion abilities of RCC cells, thereby promoting RCC metastasize to the spine. The migration and invasion of RCC cells activated by CX3CL1 are at least partially dependent on Src/FAK activation.

Key words: spinal metastasis; renal cell carcinoma; CX3CL1; CX3CR1; Src; red bone marrow

Renal cell carcinoma (RCC) is the third most common malignant tumor in the urologic system. In 2020, more than 430,000 people were diagnosed with RCC and nearly 180,000 deaths were associated with it worldwide [1]. Bone is one of the most common sites to develop metastases from RCC, just second to the lung. About one-third of patients already have bone metastasis at the time of diagnosis of RCC, and another third will develop bone metastasis over the course of the disease [2]. In terms of the location of lesions, the spine accounts for an appropriate 60% [3, 4]. The application of targeted kinase inhibitors (TKI) and immune checkpoint inhibitors brings RCC patients extended overall survival (OS), thus bone metastases become even more prevalent [2, 5]. SMs may result in pain, pathological fracture, and neurological deficits, which seriously affect the quality of life. Therefore, to develop more effective treatments, it is necessary to elucidate the molecular mechanisms underlying the SM formation among RCC patients.

The vertebral body contains a large amount of red bone marrow (RBM), which is rich in adhesion molecules and growth factors and serves as an optimal microenvironment for metastasis [6–8]. The observation of clinical cases also showed that the distribution of metastases was positively associated with the RBM content [9]. Chemokines are a group of small proteins (8–14 kDa) which are categorized into four subfamilies: CXC (α), CC (β), C (γ), and CX3C (δ) based on the protein primary structure [10]. When chemokines bind to corresponding G protein-coupled receptors, they participate in various pathological and physiological processes, such as metastasis [11, 12]. We hypothesize that some chemokines play an important role in the formation of SM from RCC.

In our previous study, we conducted a mRNA microarray to analyze SM samples from five different primary cancers (lung, breast, prostate, kidney, and liver) [13]. CX3CL1, a chemokine, was found to be involved in the process of

formation of SM from the five primary cancers. A few studies have shown that the progression of some solid cancers was promoted by CX3CL1 [14–16]. However, the role of CX3CL1 in the process of RCC metastasis to the spine is still unknown. The present study aims to verify whether CX3CL1 activates the downstream pathway by binding to its unique receptor, CX3CR1, ultimately promoting the migration and colonization of RCC cells in the spinal RBM microenvironment.

Patients and methods

Patients and samples. All of the tissue and blood samples used in the present study were collected in Zhongshan Hospital. SM tissue samples were obtained from 15 RCC patients (male/female, 10/5; age, 62.6±7.9 years) who underwent SM resection. Normal vertebral cancellous bone samples were obtained from 15 patients (male/female, 10/5; age, 67.0±5.6 years) who underwent surgery because of spinal traumatic fracture or degenerative diseases. Arterial blood samples were obtained from 30 patients (male/female, 23/7; age, 61.9±7.8 years) with SM from RCC and 30 patients (male/female, 19/11; age, 62.4±9.6 years) with spinal traumatic fracture or degenerative diseases. Limb metastasis samples were obtained from 5 patients (male/female, 5/0; age, 67.6±4.3 years) with limb metastasis from RCC. Normal limb cancellous bone samples were obtained from 5 patients (male/female, 4/1; age, 62.4±6.2 years) who underwent arthroplasty. Patients included in this study signed informed consent before surgery. The present study was approved by the Ethics Committee of Zhongshan Hospital. All procedures complied with relevant regulations.

Cell lines and culture. RCC cell lines (786O, OSRC-2, 769-P, Caki-1, ACHN) and human normal renal tubular epithelial cell line (HK-2) were purchased from the cell bank of the Chinese Academy of Sciences (Shanghai, China). All cells were cultured in RPMI-1640 medium supplemented with 10% fetal bovine serum (FBS) and 1% penicillin and streptomycin. Cells were incubated at 37 °C, 5% CO_2.

Enzyme-linked immunosorbent assay (ELISA). The serum was isolated after the arterial blood samples clotting at room temperature. The centrifugation condition was set at 1000×g for 15 min. Then, the serum samples were sub-packed and stored at –80 °C. An ELISA kit (R&D Systems, MN, USA) was used to quantify the concentration of CX3CL1 in serum according to the manufacturer's protocol.

Cell proliferation and apoptosis assay. CellTiter-Glo kit (Promega, Madison, USA) was used to determine the effects of CX3CL1 on the viability of 786O cells, which reflected the effects on proliferation. 100 µl 786O cells were seeded to a 96-well plate with a cell density of 2×10^4 cells/ml. 100 µl CellTiter-Glo solution was pipetted and added to each well based on indicated time points (0 h, 12 h, 24 h, 48 h). The cells were stimulated with 50 nM, 100 nM, and 200 nM CX3CL1 (R&D Systems, MN, USA) respectively in experimental groups. The cells without CX3CL1 treatment were used as the control group. After CellTiter-Glo solution incubation for 10 min, the luminescence was measured using a microplate luminometer (Thermo Fisher Scientific, Inc., MA, USA). Cell apoptosis rate was measured using an Annexin V-fluorescein isothiocyanate/propidium iodide apoptosis kit (BD Biosciences, NJ, USA) according to the manufacturer's protocol. Based on a previous study [16], the 786O cells were stimulated by 50 nM CX3CL1. Apoptosis rate was detected at 0 h, 24 h, and 48 h after stimulation using the flow cytometer (BD Biosciences, NJ, USA).

Wound-healing assay. Cells were equivalently seeded into a 6-well plate and cultured to 90–100% confluence. Then the cells were scratched across the center of the well with a sterile plastic pipette tip. Each well was gently washed by PBS for twice to remove the detached cells. Cells were treated with CX3CL1 (50 nM) or CX3CL1+neutralizing antibody (50 nM; Abcam, Cambridge, UK; cat. no. ab89229). The group without CX3CL1 stimulation was set as control. Images were captured at 0 h and 24 h. The wound closure areas were measured and calculated as a percentage of cell migration into the wound at 24 h compared to the area at 0 h.

Transwell migration and invasion assays. The 24-well Transwell permeable supports with 8.0 µm pores (Corning-Costar, NY, USA) were used to detect the migratory ability of RCC cells. The upper chambers pre-coated with matrigel were used to perform the invasion assay. Cells were harvested and re-suspended in RPMI-1640 without FBS. Each lower chamber was filled with 550 µl RPMI-1640 medium supplemented with 1% FBS, followed by adding CX3CL1 (50 nM) or CX3CL1+neutralizing antibody (50 nM; cat. no. ab89229). The group without CX3CL1 stimulation was set as control. The Transwell assay was also used to evaluate the motility and invasion of 786O cells treated with signaling molecules inhibitors. 5×10^4 cells were seeded into each upper chamber. After incubation at 37 °C for 24 h, the cells remaining in the upper chamber were carefully cleaned using a cotton swab. The cells on the lower surface of the polycarbonate membrane were fixed with 4% paraformaldehyde and stained with crystal violet. Images were captured at 100× magnification. The number of cells was counted and averaged in four randomly selected fields.

Western blot. After washing with phosphate-buffered saline (PBS), cells were lysed by RIPA lysis buffer containing Protease and phosphatase inhibitor cocktail (Cell Signaling Technology, MA, USA). Tissue samples underwent liquid nitrogen grinding before RIPA lysis. The protein samples were resolved by sodium dodecyl sulfate-polyacrylamide gel electrophoresis (SDS-PAGE). Then, the proteins were electrophoretically transferred to the polyvinylidene difluoride (PVDF) membrane (Millipore, MA, USA). Tris-buffered saline containing 5% skim milk was used to block the membrane. The membrane was immunoblotted with anti-CX3CR1 primary antibody (1:200; Santa Cruz Biotechnology, TX, USA; cat. no. sc-377227), anti-CX3CL1 primary antibody (1:1000; Abcam, Cambridge, UK; cat. no.

ab89229), and anti-tubulin primary antibody (1:5000; BBI Life Sciences, Sangon Biotech; cat. no. D191046) at 4 °C overnight. For the analysis of signaling induced by CX3CL1/CX3CR1, RCC cells were stimulated with 50 nM CX3CL1 (R&D Systems, MN, USA) and detected at indicated time points (0, 15, 30, 45, 60, 120 min). In the blocking experiment, 786O cells were pre-treated with 1 μM Bosutinib (inhibitor of Src; Selleck, TX, USA) or/and PF-00562271 (inhibitor of FAK; Selleck, TX, USA) for 60 min, followed by stimulation with 50 nM CX3CL1 for 45 min. The membrane loaded with target proteins were incubated with primary antibodies of both the total and phosphorylated forms of Src (Src, 1:1000, cat. no. 2108; phospho-Src, 1:1000, cat. no. 6943; Cell Signaling Technology, MA, USA) and FAK (FAK, 1:1000, cat. no. 3285; phospho-FAK, 1:500, cat. no. 3281; Cell Signaling Technology). Anti-GAPDH antibody (1:5000; BBI Life Sciences, Sangon Biotech; cat. no. D190636) was used to detect GAPDH as the internal reference. Goat anti-rabbit (cat. no. D110058) or anti-mouse (cat. no. D110087) secondary antibodies conjugated with horseradish peroxidase (1:5000; BBI Life Sciences, Sangon Biotech) were used to recognize the corresponding primary antibody. The blots were detected using immobilon western HRP substrate (Millipore, MA, USA).

Immunohistochemistry staining. The tissue samples were fixed with 4% polyoxymethylene, decalcified by EDTA, dehydrated using graded ethanol, embedded in paraffin, and then sectioned to 4 μm thickness. Antigen retrieval was performed using citrate buffer and microwave. Sections were treated with 3% H_2O_2 for 15 min and washed in tris-buffered saline (TBS) twice. 5% bovine serum albumin (BSA) was used for blocking, followed by incubation with anti-CX3CL1 primary antibody (1:200; Abcam; cat. no. ab25088) and anti-CX3CR1 primary antibody (1:200; Abcam; cat. no. ab8021) at 4 °C overnight. Then the sections were incubated with relevant secondary antibody (BBI Life Sciences, Sangon Biotech) at room temperature for 1 h. 3,3'-diaminobenzidine buffer (DAKO, CA, USA) staining and hematoxylin counterstaining were performed in turn.

Statistical analysis. Measurement data were presented as mean ± SD. Statistical analysis was performed using GraphPad Prism 8.0 (GraphPad Software, CA, USA). Student's t-test was used to determine the statistical significance between the two groups as noted in the figure legends. For three or more groups, one-way ANOVA test followed by Bonferroni test was performed for multiple comparisons. The correlations between serum CX3CL1 levels with the number of metastatic sites were determined using Pearson's correlation coefficient (r). Statistical significance was set as $p<0.05$.

Results

The expression of CX3CL1/CX3CR1 in the tissue samples, serum, and cell lines. Immunohistochemical staining demonstrated that SMs had a higher expression level of CX3CR1 compared to limb metastases (Figure 1A). CX3CL1 was highly expressed in the marrow of the normal vertebral cancellous bone, whereas lower expression in the normal limb cancellous bone (Figure 1B). The expression level of CX3CR1 appeared to be low in both vertebrae and limb bone (Figure 1C). Western blotting of tissue samples was performed. The results verified higher expression levels of CX3CL1 and CX3CR1 in normal vertebral marrow and vertebral metastasis, respectively (Figures 1D, 1E). ELISA demonstrated that the concentration of CX3CL1 was higher in serum samples of patients with SMs (Figure 1F). We examined the association of serum CX3CL1 levels with the number of SMs, which were detected by PET/CT scan. Serum CX3CL1 levels were positively associated with the number of SMs (Figure 1G). As shown in Figure 2A, we examined the expression level of CX3CR1 in RCC cell lines using western blot. All of the cell lines used express CX3CR1 to a different degree. 786O cells and OSRC-2 expressed the highest level of CX3CR1 (Figure 2A).

CX3CL1 doesn't inhibit the survival of 786O cells. The CellTiter-Glo assay was used to detect the effects of CX3CL1 on the proliferation of 786O cells. The results of the CellTiter-Glo assay showed that the indicated concentrations (50 nM, 100 nM, 200 nM) of CX3CL1 neither promote nor inhibit proliferation of 786O cells over 48 h (Figure 2B). Flow cytometry was used to analyze the effects of CX3CL1 on the apoptosis of 786O cells. The apoptosis rate at 0 h, showed as significantly higher than that at 24 h and 48 h after stimulation (Figure 2C).

CX3CL1 promotes the mobility and invasion of RCC cells. Scratch wound-healing assay indicated that stimulation with 50 nM CX3CL1 could significantly promote wound healing after 24 h, and the CX3CL1 neutralizing antibody prevented the effects promoted by CX3CL1 (Figures 3A, 3B). As shown in Figures 3C and 3D, Transwell migration and invasion were performed. Cell migration number significantly increased after treatment with 50 nM CX3CL1. Similar to Transwell migration, the presence of 50 nM CX3CL1 also significantly increased the number of invaded cells. However, both the migration and the invasion ability promoted by CX3CL1 were prevented by the CX3CL1 neutralizing antibody. For further functional validation, wound healing and Transwell assays were used to analyze the effect of CX3CL1 on migration and invasion ability of another cell line OSRC-2. CX3CL1 also promoted the migration and invasion of OSRC-2 cells (Supplementary Figures S1A–S1C).

CX3CL1 activates the Src/FAK signaling pathway in RCC cells. The phosphorylation level of Src and FAK in 786O cells stimulated by CX3CL1 was assessed using western blotting at indicated time points (0, 15, 30, 45, 60, 120 min). The quantification was performed using the ratio of the gray value of phosphorylated proteins to total proteins. The phosphorylation of Src began to increase at 15 min after stimulation, reached the peak at 45 min, and then subsided

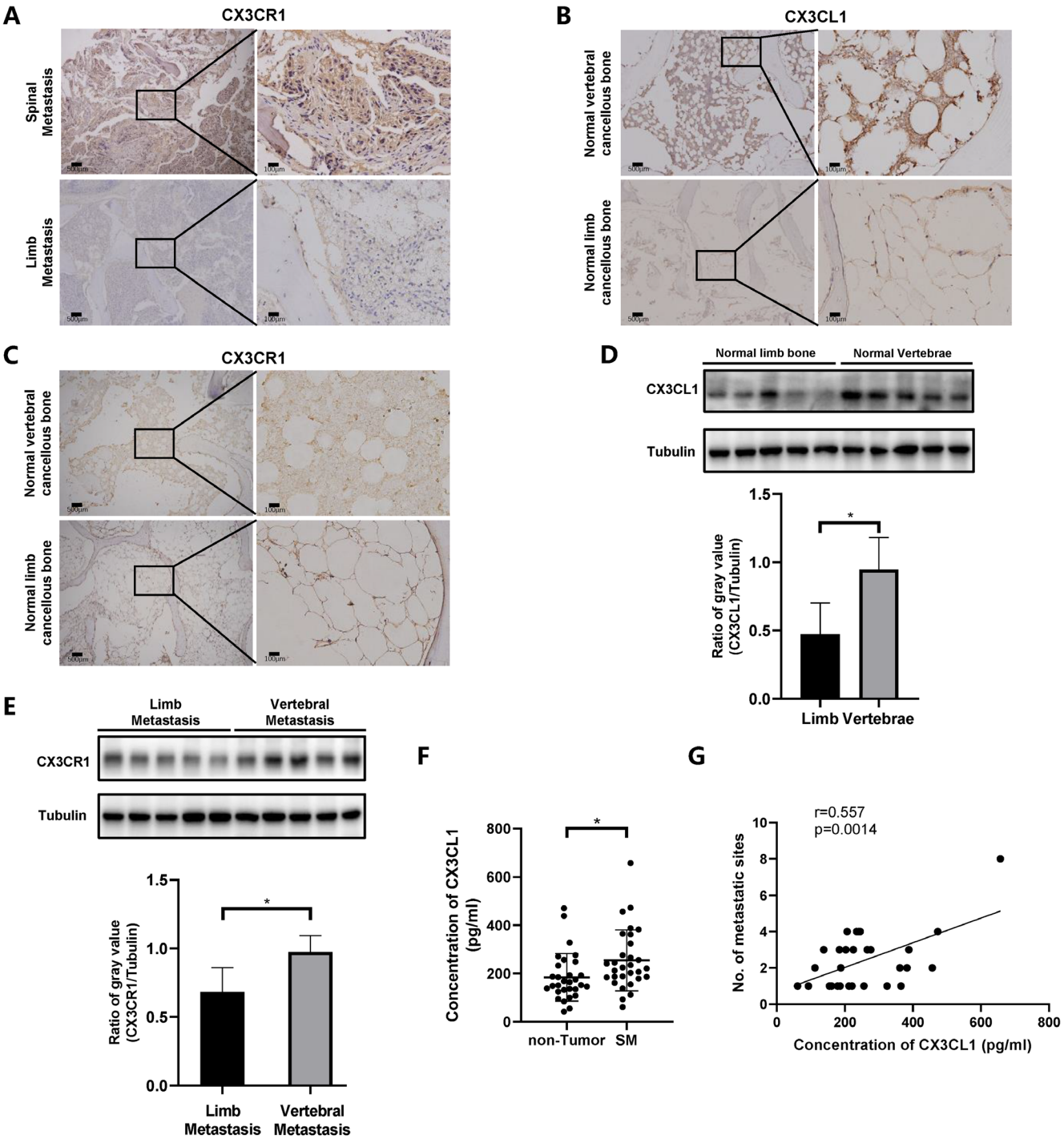

Figure 1. The expression of CX3CR1 and CX3CL1 in the tissue sample and serum. A) Representative immunohistochemical staining of CX3CR1 in SM and limb metastasis. B) Representative immunohistochemical staining of CX3CL1 in the marrow of the normal vertebral cancellous bone and normal limb cancellous bone. C) Representative immunohistochemical staining of CX3CR1 in the marrow of the normal vertebral cancellous bone and normal limb cancellous bone. D, E) Western blotting was performed to analyze the expression level of CX3CL1 and CX3CR1 in vertebral marrow and vertebral metastasis respectively. Representative western blotting images were shown and the experiment was conducted three times independently. F) The concentrations of CX3CL1 in serum samples (n=30/group) were detected by ELISA. G) The association of serum CX3CL1 levels with the number of SMs; p-value was calculated using Student's t-test, *p<0.05

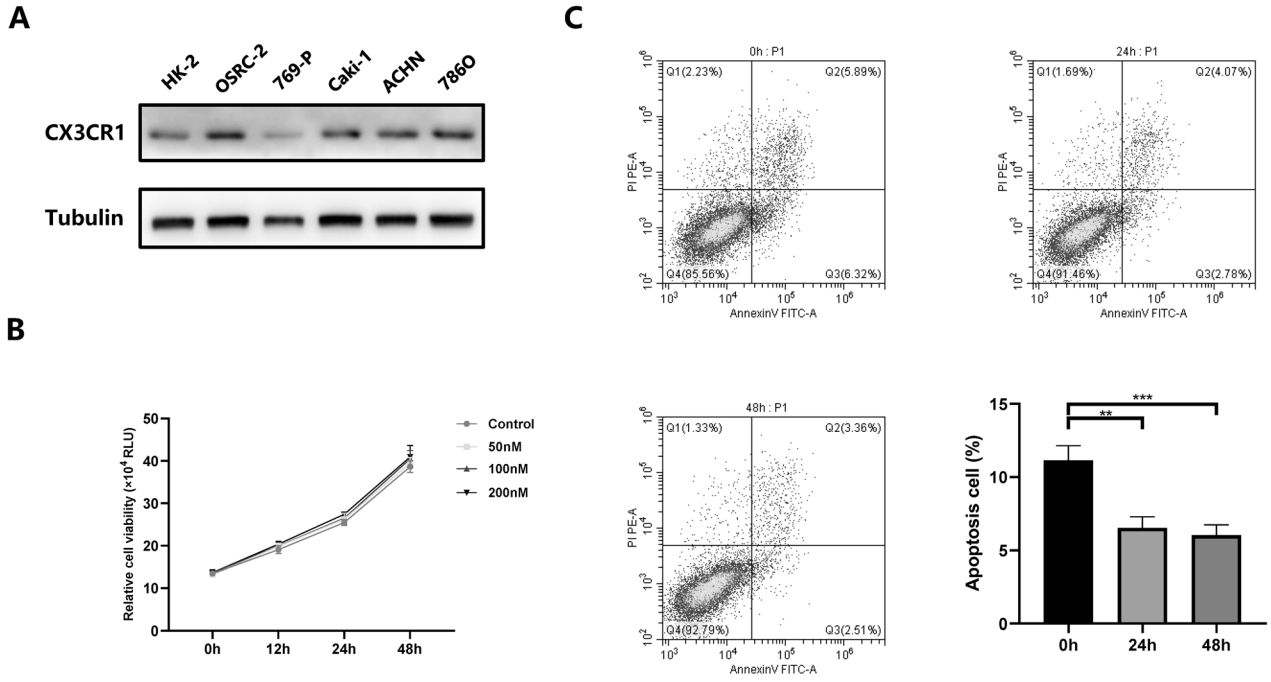

Figure 2. The expression of CX3CR1 in cell line and cell viability and apoptosis assay. A) The expression of CX3CR1 in RCC cell lines. B) The effects of different concentrations (50 nM, 100 nM, 200 nM) of CX3CL1 on 786O cells' viability over 48 h. C) The apoptosis rate at 0 h, 24 h, and 48 h after 50 nM CX3CL1 stimulation. Each experiment was conducted three times independently and representative images were shown. One-way ANOVA with a post hoc Bonferroni test was used to determine statistical difference.

to baseline level gradually. The phosphorylation of FAK began to increase 15 min, reached the peak at 45 min, and continued through 120 min (Figures 4A, 4B). Similar results were also found in OSRC-2 cells, as presented in Supplementary Figures S2A and S2B. The role of Src and FAK in the signaling pathway induced by CX3CL1/CX3CR1 was examined using kinase inhibitors. 786O cells were pretreated with the inhibitors of 1 μM Bosutinib or/and PF-00562271 for 60 minutes and then stimulated by CX3CL1 for 45 min. Western blotting showed that Bosutinib and PF-00562271 reduced the phosphorylation of Src and FAK, respectively (Figures 4C, 4D).

Targeted inhibition of Src/FAK suppresses the increased motility and invasion of 786O cells triggered by CX3CL1/CX3CR1. In order to evaluate the mobility of 786O cells stimulated with CX3CL1, 786O cells were pretreated with 1 μM Bosutinib or/and PF-00562271, and stimulated by 50 nM CX3CL1. Then cells were fixed and stained with TRITC-Phalloidin (red) and DAPI (blue). Confocal images of 786O cells treated with CX3CL1 showed that F-actin structures increased. However, treatment with Bosutinib and (or) PF-00562271 induced stress fiber decreased (Figure 5A). For further validation, transwell migration and invasion were performed to analyze the motility and invasion of 786O cells after targeted inhibition of Src/FAK. The data showed that inhibition of Src/FAK could rescue the increased motility and invasion of 786O cells triggered by the CX3CL1/CX3CR1 axis (Figures 5B–5E).

Discussion

Prostate, kidney, lung, and breast cancer are primary cancers that most often lead to bone metastasis [17]. The spine is the most common site of bone metastasis [18, 19]. SM may cause pain, instability, and neurological injuries. It was reported that 28% of patients who developed bone metastases from RCC experienced spinal cord or/and nerve root compression [5]. In the process of tumor invasion of the bone marrow, on one hand, cancer cells can produce some growth factors to promote osteoblastic or osteolytic activity; on the other hand, bone remodeling can also release some growth factors to promote cancer progression, thereby forming a vicious circle. The abundant RBM of vertebrae is a very important factor, which makes the spine the predilection site of metastasis. Due to excessive blood flow, the abundance of adhesion molecules and growth factors, RBM is an ideal metastatic niche [6, 8, 20]. Caracappa et al. [21] used different ways to calculate the RBM mass in various bone segments. Spine, especially the thoracic spine and lumbar spine, has much more RBM than limb bones such as femora, humeri, and clavicles. Onken et al. conducted a study

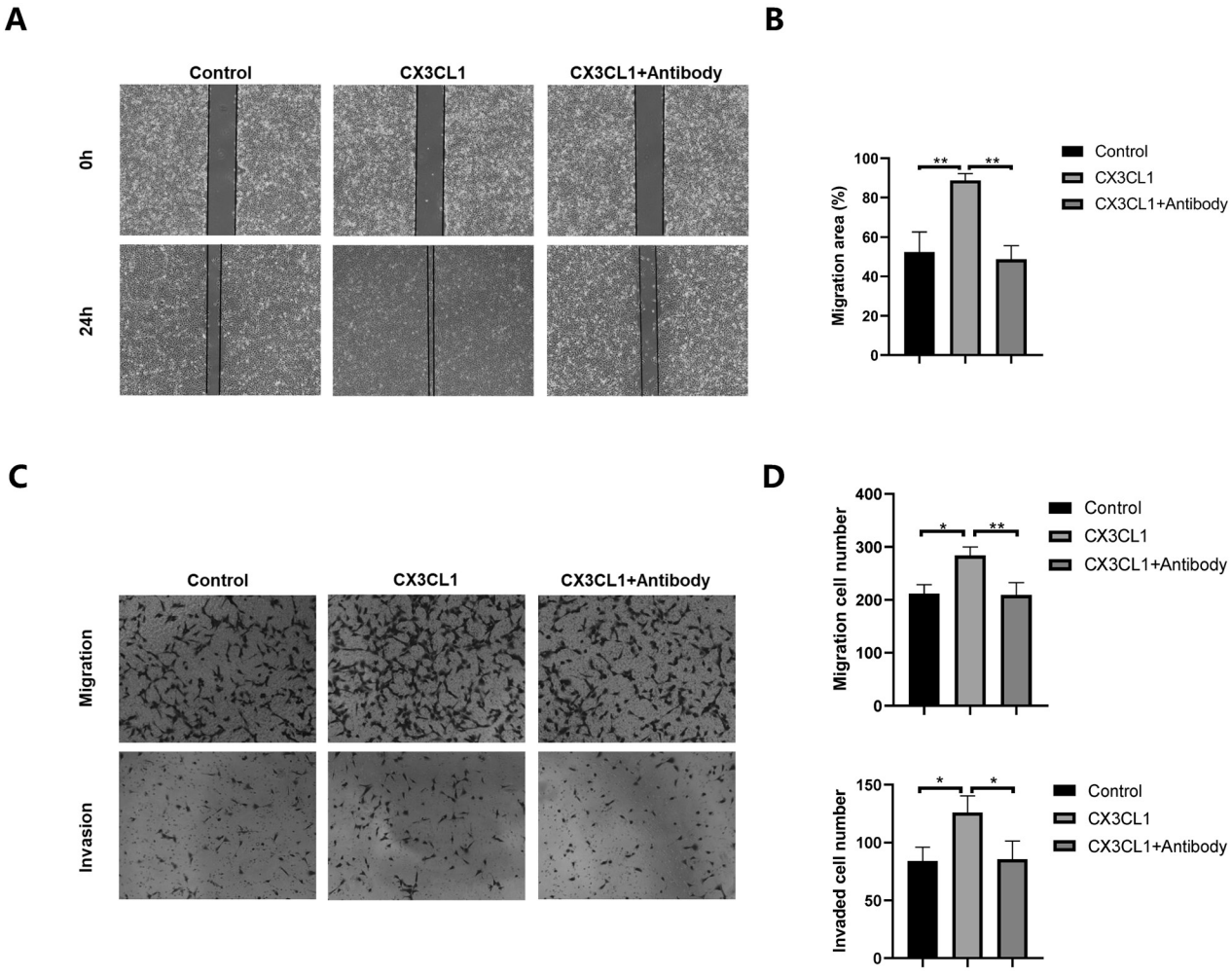

Figure 3. CX3CL1 promotes the migration and invasion abilities of 786O cells. A, B) Wound-healing assays of 786O cells treated with 50 nM CX3CL1 or 50 nM CX3CL1+neutralizing antibody (×100 magnification). C, D) The Transwell migration and invasion assays of 786O cells treated with 50 nM CX3CL1 or 50 nM CX3CL1+neutralizing antibody (×100 magnification). Each experiment was conducted three times independently and representative images were shown. Statistical significance between the two groups was determined by one-way ANOVA with a post hoc Bonferroni test, *p<0.05, **p<0.01

that shows that the incidence of bone metastases and RBM content of the corresponding bone is mostly proportional [9]. Based on the above discussion, it would be reasonable to speculate that the microenvironment of RBM promotes RCC to metastasize to the spine.

In 1889, Paget [22] hypothesized that cancer cells (defined as seeds) tend to metastasize to a favorable microenvironment (defined as soil). It is well known that metastasis is not a random process, instead, an organ-specific process. Metastasis often occurs in certain organs, such as lung, liver, bone marrow, and brain, while other organs, such as kidney, pancreas, and skin rarely undergo metastasis [23]. Chemokines are a subgroup of cytokines. They are low-molecular-weight proteins that are involved in regulating the migration of white blood cells and other cells that affect the inflammatory process [24]. Although metastasis is a complicated process involving multiple factors and small molecule regulators, many studies have shown that chemokines and their corresponding receptors play a crucial role in metastasis [25]. The altered expression of chemokines and their receptors is found in many malignancies and subsequently leads to abnormal signal transduction. Bone-homing tumor cells overexpress chemokine receptors, whose ligand is secreted by stromal cells, including BMSC.

In our previous study, we analyzed cancellous bone with and without metastases in the spine using mRNA microarray [13]. CX3CL1 was identified to be one of the potential chemokines involved in the process of SMs formation. CX3CR1 is the unique receptor of CX3CL1. CX3CL1 has a dual function to act as a chemoattractant and an adhesion molecule by interacting with CX3CR1. We confirmed the CX3CR1 expression in RCC cell lines and SMs in the present study.

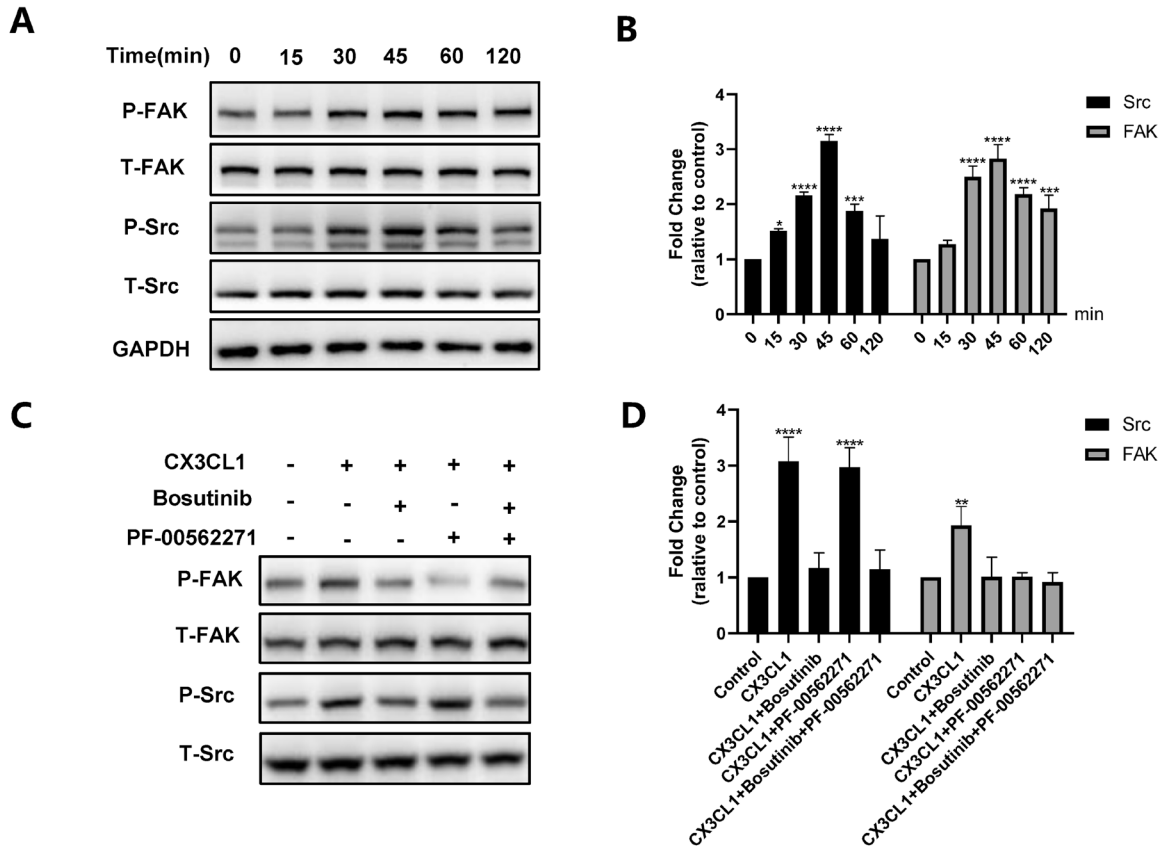

Figure 4. CX3CL1 activates the Src/FAK signaling pathway in RCC cells. A, B) Phosphorylation levels of Src and FAK of 786O cells after stimulated by CX3CL1 for indicated time points. 0 min as control. Fold changes were determined by averaging the ratios relative to the control group. C, D) 786O cells were pretreated with Bosutinib or/and PF-00562271 and then stimulated by CX3CL1. The phosphorylation levels of Src and FAK were detected. The group without CX3CL1 and inhibitors treatment as control. Fold changes were determined by averaging the ratios relative to the control group. Each experiment was conducted three times independently and representative images were shown. Statistical significance was determined by one-way ANOVA with a post hoc Bonferroni test. **p<0.01, ***p<0.001, ****p<0.0001

Previous studies have reported that CX3CR1 is expressed in several types of cancers, such as prostate cancer [14], breast cancer [15], RCC [16], pancreatic cancer [26], ovarian cancer [27], and colon cancer [28]. These authors showed that CX3CL1 promotes the metastasis of these cancers. However, CX3CL1 did not always promote cancer progression. Sciumè et al. [29] analyzed the expression level and function of the CX3CL1/CX3CR1 axis in human glioma cells. The results showed that endogenous CX3CL1 promotes tumor cell aggregation, thereby negatively regulating tumor invasion. In addition, inhibition of CX3CL1 expression by TGF-β1 might contribute to tumor cell invasion. Our present study found that CX3CL1 neither inhibited the proliferation of 786O cells nor promoted the apoptosis of RCC cells. It is consistent with our previous study about breast cancer [30]. CX3CL1 even showed a function of inhibiting cellular apoptosis.

As for the mechanism, we detected the phosphorylation of Src and FAK. Activation of the Src/FAK signaling pathway leads to cytoskeleton reorganization, which has an important impact on cell migration [31]. We first reported CX3CL1 promotes the migration and invasion of RCC cell lines through the Src/FAK signaling pathway. Although Yao et al. [16] previously reported that CX3CL1 increased the migration ability of RCC cells using wound healing assay, they did not analyze the invasion ability of RCC cells. In the present study, we focused on the SM and conducted more functional experiments than Yao's study to analyze the invasion ability as well as migration ability of RCC cells. What's more, we found a new underlying signaling mechanism that promotes RCC to metastasize to the spine. Both Src and FAK are non-receptor tyrosine kinases, involved in cell differentiation, survival, adhesion, and migration [32, 33]. When phosphorylation occurs at Tyr416, the enzyme activity of Src increases. Phosphorylated Src binds to FAK at Tyr397, thereby phosphorylating FAK at Tyr576/577 [32]. Bosutinib (inhibitor of Src) and PF-00562271 (inhibitor of FAK) inhibited the mobility and invasion of RCC cells, suggesting that drugs targeting Src/FAK have potential value in patients with

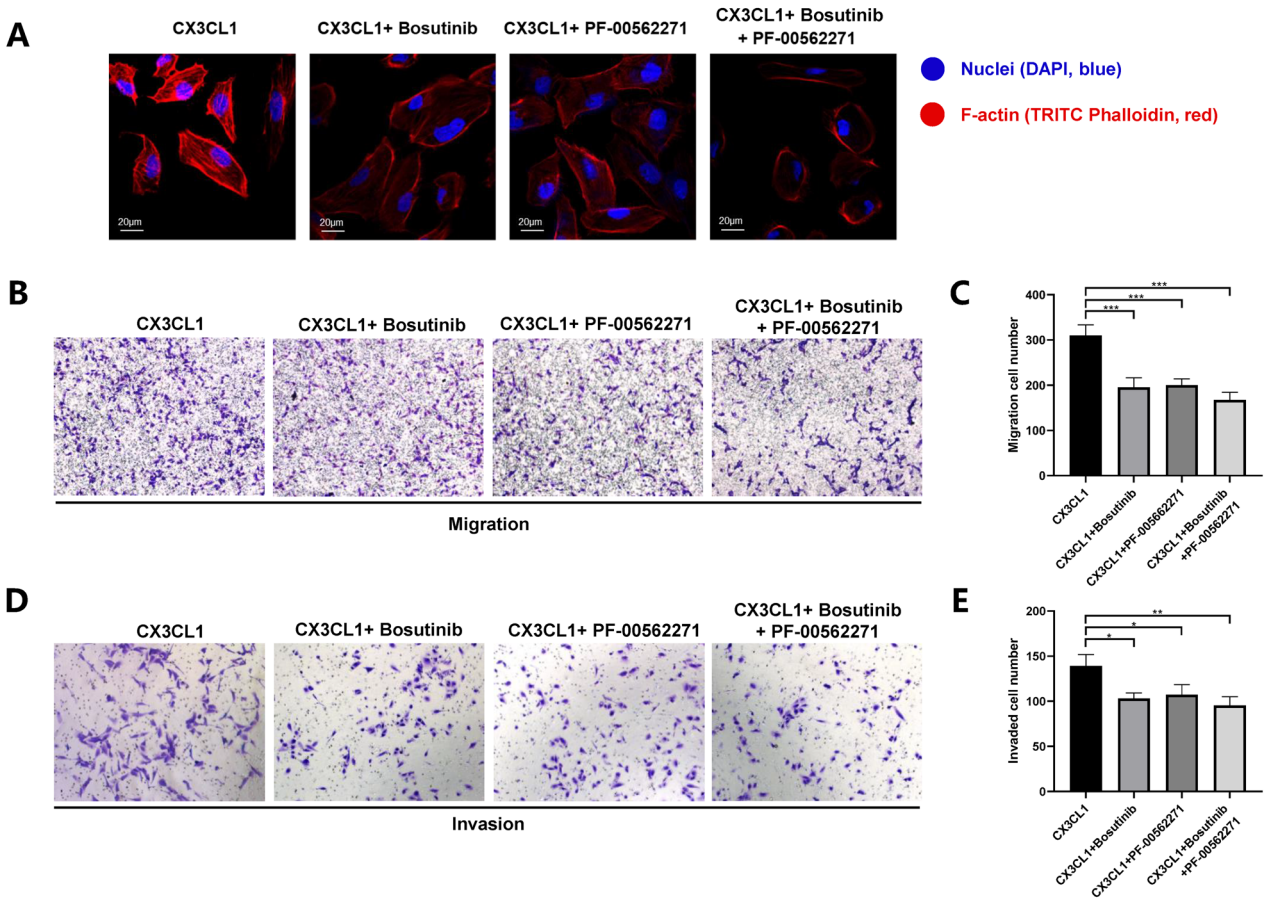

Figure 5. Targeted inhibition of Src/FAK suppresses the increased motility and invasion of 786O cells triggered by CX3CL1/CX3CR1. A) CX3CL1 promoted F-actin formation, whereas Bosutinib and (or) PF-00562271 decreased F-actin structure. Cells were stained with TRITC-Phalloidin (red) and DAPI (blue). B, C) The migration assays of 786O cells stimulated by CX3CL1 with or without inhibitors (×100 magnification). D, E) The invasion assays of 786O cells stimulated by CX3CL1 with or without inhibitors (×100 magnification). Each experiment was conducted three times independently and representative images were shown. The cell number of migration and invasion between the two groups were compared using one-way ANOVA with a post hoc Bonferroni test. *p<0.05, **p<0.01, ***p<0.001

SM from RCC. The ongoing and completed clinical trials of Bosutinib and PF-00562271 mainly focused on leukemia, breast cancer, and prostate cancer, excluding advanced RCC [33, 34]. Our findings may provide evidence for the use of these drugs in treating patients with SM from RCC.

In conclusion, the present study indicated that CX3CL1 in RBM of spinal cancellous bone enhances migration and invasion abilities of RCC cells, thereby promoting RCC to metastasize to the spine. The migration and invasion of RCC cells activated by CX3CL1 are at least partially dependent on Src/FAK activation.

Supplementary information is available in the online version of the paper.

Acknowledgments: This study was sponsored by the National Natural Science Foundation of China (grant number: 81572629, 82002841).

References

[1] SUNG H, FERLAY J, SIEGEL RL, LAVERSANNE M, SOERJOMATARAM I et al. Global Cancer Statistics 2020: GLOBOCAN Estimates of Incidence and Mortality Worldwide for 36 Cancers in 185 Countries. CA Cancer J Clin 2021; 71: 209–249. https://doi.org/10.3322/caac.21660

[2] WOOD SL, BROWN JE. Skeletal metastasis in renal cell carcinoma: current and future management options. Cancer Treat Rev 2012; 38: 284–291. https://doi.org/10.1016/j.ctrv.2011.06.011

[3] WONG DA, FORNASIER VL, MACNAB I. Spinal metastases: the obvious, the occult, and the impostors. Spine 1990; 15: 1–4.

[4] RUATTA F, DEROSA L, ESCUDIER B, COLOMBA E, GUIDA A et al. Prognosis of renal cell carcinoma with bone metastases: Experience from a large cancer centre. Eur J Cancer 2019; 107: 79–85. https://doi.org/10.1016/j.ejca.2018.10.023

[5] WOODWARD E, JAGDEV S, MCPARLAND L, CLARK K, GREGORY W et al. Skeletal complications and survival in renal cancer patients with bone metastases. Bone 2011; 48: 160–166. https://doi.org/10.1016/j.bone.2010.09.008

[6] CROUCHER PI, MCDONALD MM, MARTIN TJ. Bone metastasis: the importance of the neighbourhood. Nat Rev Cancer 2016; 16: 373–386. https://doi.org/10.1038/nrc.2016.44

[7] WANG N, DOCHERTY FE, BROWN HK, REEVES KJ, FOWLES AC et al. Prostate cancer cells preferentially home to osteoblast-rich areas in the early stages of bone metastasis: evidence from in vivo models. J Bone Miner Res 2014; 29: 2688–2696. https://doi.org/10.1002/jbmr.2300

[8] ZHANG Y, HE W, ZHANG S. Seeking for Correlative Genes and Signaling Pathways with Bone Metastasis from Breast Cancer by Integrated Analysis. Front Oncol 2019; 9: 138. https://doi.org/10.3389/fonc.2019.00138

[9] ONKEN JS, FEKONJA LS, WEHOWSKY R, HUBERTUS V, VAJKOCZY P. Metastatic dissemination patterns of different primary tumors to the spine and other bones. Clin Exp Metastasis 2019; 36: 493–498. https://doi.org/10.1007/s10585-019-09987-w

[10] ZLOTNIK A, YOSHIE O. Chemokines: a new classification system and their role in immunity. Immunity 2000; 12: 121–127. https://doi.org/10.1016/s1074-7613(00)80165-x

[11] MOLLICA PV, MASSARA M, CAPUCETTI A, BONECCHI R. Chemokines and Chemokine Receptors: New Targets for Cancer Immunotherapy. Front Immunol 2019; 10: 379. https://doi.org/10.3389/fimmu.2019.00379

[12] MARCUZZI E, ANGIONI R, MOLON B, CALI B. Chemokines and Chemokine Receptors: Orchestrating Tumor Metastasization. Int J Mol Sci 2018; 20. https://doi.org/10.3390/ijms20010096

[13] LIU W, BIAN C, LIANG Y, JIANG L, QIAN C et al. CX3CL1: a potential chemokine widely involved in the process spinal metastases. Oncotarget 2017; 8: 15213–15219. https://doi.org/10.18632/oncotarget.14773

[14] JAMIESON WL, SHIMIZU S, D'AMBROSIO JA, MEUCCI O, FATATIS A. CX3CR1 is expressed by prostate epithelial cells and androgens regulate the levels of CX3CL1/fractalkine in the bone marrow: potential role in prostate cancer bone tropism. Cancer Res 2008; 68: 1715–1722. https://doi.org/10.1158/0008-5472.CAN-07-1315

[15] TARDAGUILA M, MIRA E, GARCIA-CABEZAS MA, FEIJOO AM, QUINTELA-FANDINO M et al. CX3CL1 promotes breast cancer via transactivation of the EGF pathway. Cancer Res 2013; 73: 4461–4473. https://doi.org/10.1158/0008-5472.CAN-12-3828

[16] YAO X, QI L, CHEN X, DU J, ZHANG Z et al. Expression of CX3CR1 associates with cellular migration, metastasis, and prognosis in human clear cell renal cell carcinoma. Urol Oncol 2014; 32: 162–170. https://doi.org/10.1016/j.urolonc.2012.12.006

[17] JAYARANGAIAH A, KEMP AK, THEETHA KARIYANNA P. Bone Metastasis. In: StatPearls. StatPearls Publishing; 2019. https://www.ncbi.nlm.nih.gov/books/NBK507911/

[18] OSORIO M, MOUBAYED SP, SU H, URKEN ML. Systematic review of site distribution of bone metastases in differentiated thyroid cancer. Head Neck 2017; 39: 812–818. https://doi.org/10.1002/hed.24655

[19] ZHOU Y, YU QF, PENG AF, TONG WL, LIU JM et al. The risk factors of bone metastases in patients with lung cancer. Sci Rep 2017; 7: 8970. https://doi.org/10.1038/s41598-017-09650-y

[20] D'ORONZO S, COLEMAN R, BROWN J, SILVESTRIS F. Metastatic bone disease: Pathogenesis and therapeutic options: Up-date on bone metastasis management. J Bone Oncol 2019; 15: 4. https://doi.org/10.1016/j.jbo.2018.10.004

[21] CARACAPPA PF, CHAO TC, XU XG. A study of predicted bone marrow distribution on calculated marrow dose from external radiation exposures using two sets of image data for the same individual. Health Phys 2009; 96: 661–674. https://doi.org/10.1097/01.HP.0000346304.45813.36

[22] PAGET S. The distribution of secondary growths in cancer of the breast. 1889. Cancer Metastasis Rev 1989; 8: 98–101.

[23] ZLOTNIK A, BURKHARDT AM, HOMEY B. Homeostatic chemokine receptors and organ-specific metastasis. Nat Rev Immunol 2011; 11: 597–606. https://doi.org/10.1038/nri3049

[24] PALOMINO DC, MARTI LC. Chemokines and immunity. Einstein 2015; 13: 469–473. https://doi.org/10.1590/S1679-45082015RB3438

[25] SARVAIYA PJ, GUO D, ULASOV I, GABIKIAN P, LESNIAK MS. Chemokines in tumor progression and metastasis. Oncotarget 2013; 4: 2171–2185. https://doi.org/10.18632/oncotarget.1426

[26] CELESTI G, DI CARO G, BIANCHI P, GRIZZI F, MARCHESI F et al. Early expression of the fractalkine receptor CX3CR1 in pancreatic carcinogenesis. Br J Cancer 2013; 109: 2424–2433. https://doi.org/10.1038/bjc.2013.565

[27] KIM M, ROOPER L, XIE J, KAJDACSY-BALLA AA, BARBOLINA MV. Fractalkine receptor CX(3)CR1 is expressed in epithelial ovarian carcinoma cells and required for motility and adhesion to peritoneal mesothelial cells. Mol Cancer Res 2012; 10: 11–24. https://doi.org/10.1158/1541-7786.MCR-11-0256

[28] ZHENG J, YANG M, SHAO J, MIAO Y, HAN J et al. Chemokine receptor CX3CR1 contributes to macrophage survival in tumor metastasis. Mol Cancer 2013; 12: 141. https://doi.org/10.1186/1476-4598-12-141

[29] SCIUME G, SORIANI A, PICCOLI M, FRATI L, SANTONI A et al. CX3CR1/CX3CL1 axis negatively controls glioma cell invasion and is modulated by transforming growth factor-beta1. Neuro Oncol 2010; 12: 701–710. https://doi.org/10.1093/neuonc/nop076

[30] LIANG Y, YI L, LIU P, JIANG L, WANG H et al. CX3CL1 involves in breast cancer metastasizing to the spine via the Src/FAK signaling pathway. J Cancer 2018; 9: 3603–3612. https://doi.org/10.7150/jca.26497

[31] HAMAGUCHI M, YAMAGATA S, THANT AA, XIAO H, IWATA H et al. Augmentation of metalloproteinase (gelatinase) activity secreted from Rous sarcoma virus-infected cells correlates with transforming activity of src. Oncogene 1995; 10: 1037–1043.

[32] BRUNTON VG, FRAME MC. Src and focal adhesion kinase as therapeutic targets in cancer. Curr Opin Pharmacol 2008; 8: 427–432. https://doi.org/10.1016/j.coph.2008.06.012

[33] PATEL A, SABBINENI H, CLARKE A, SOMANATH PR. Novel roles of Src in cancer cell epithelial-to-mesenchymal transition, vascular permeability, microinvasion and metastasis. Life Sci 2016; 157: 52–61. https://doi.org/10.1016/j.lfs.2016.05.036

[34] LEE BY, TIMPSON P, HORVATH LG, DALY RJ. FAK signaling in human cancer as a target for therapeutics. Pharmacol Ther 2015; 146: 132–149. https://doi.org/10.1016/j.pharmthera.2014.10.001

https://doi.org/10.4149/neo_2022_211205N1728

CX3CL1 in the red bone marrow promotes renal cell carcinoma to metastasize to the spine by involving the Src-related pathway

An-Nan HU#, Fan-Cheng CHEN#, Ke-Tao WANG#, Zhen-Qing WANG, Yun LIANG, Jian DONG*

Supplementary Information

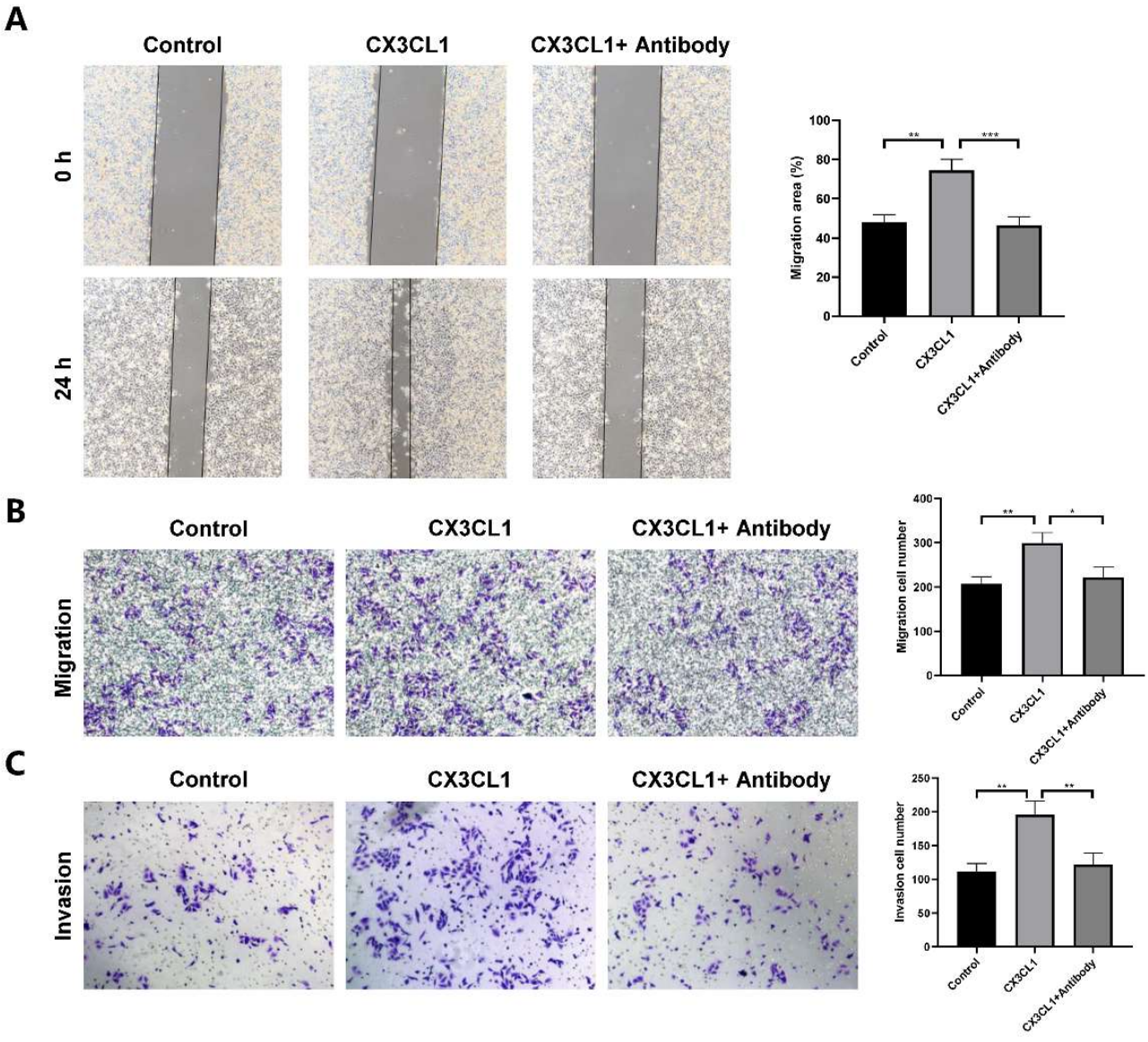

Supplementary Figure S1. CX3CL1 promotes the migration and invasion abilities of OSRC-2 cells. A) Wound healing assays of OSRC-2 cells treated with 50 nM CX3CL1 or 50 nM CX3CL1+neutralizing antibody. (×100 magnification). B) The transwell migration and invasion assays of OSRC-2 cells treated with 50 nM CX3CL1 or 50 nM CX3CL1+neutralizing antibody. (×100 magnification). Each experiment was conducted three times independently and representative images were shown. Statistical significance between two groups was determined by one-way ANOVA with a post hoc Bonferroni test. *p<0.05, **p<0.01, ***p<0.001

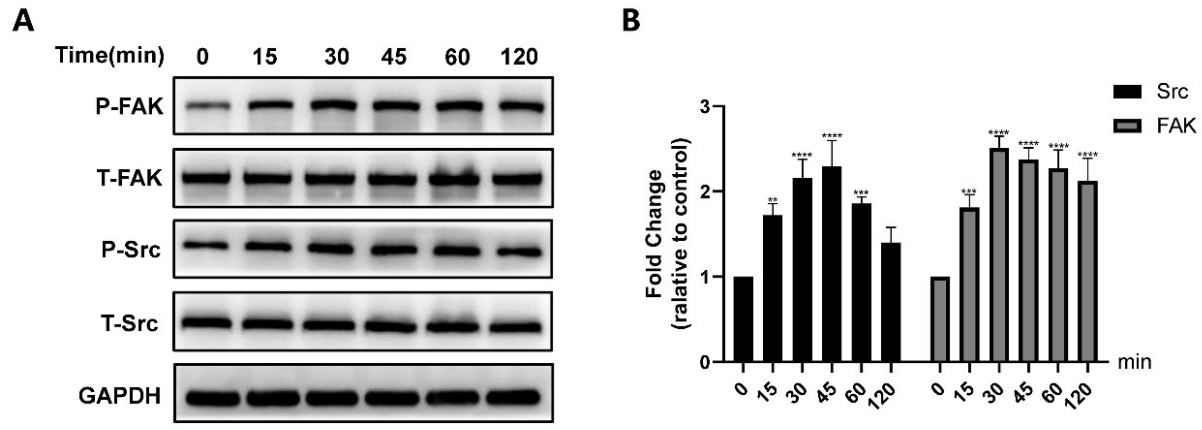

Supplementary Figure S2. CX3CL1 activates the Src/FAK signaling pathway in OSRC-2 cells. A) Phosphorylation levels of Src and FAK of OSRC-2 cells after stimulation of CX3CL1 at indicated time points. 0 min as control. B) Fold changes were determined by averaging the ratios relative to control group. Each experiment was conducted three times independently and representative images were shown. Statistical significance between two groups was determined by one-way ANOVA with a post hoc Bonferroni test. **p<0.01, ***p<0.001, ****p<0.001